The effects already found are so large as to suggest that tetrachromatic matching does not provide a satisfactory answer to the problem of nonadditivity in large-field color matching. In so far as the rods do intrude, the fourth stimulus must take care of their activity. However, complete physiological identities would require even more stimuli. An obvious suggestion is to use seven, three each for the fovea and para-fovea and one for the rods. Where the limit to this proliferation might lie for a practical compromise is a difficult question. Lozano and Palmer[5] have suggested that the CIE 1964 color-matching functions may serve adequately enough for large-field colorimetry.

I thank Dr. W. S. Stiles for his helpful advice and criticism. The subjects' patience and careful observations are gratefully acknowledged.

[1]P. W. Trezona, "The tetrachromatic colour match as a colorimetric technique," Vision Res. 13, 9–25 (1973).
[2]P. W. Trezona, "Additivity in the tetrachromatic colour matching system," Vision Res. 14, 1291–1303 (1974).
[3]F. J. J. Clarke, "Needs and prospects for a tetrachromatic system of large field colorimetry," *AIC Second Congress: Colour* 73 (Adam Hilger, London, 1974), pp. 319–324.
[4]F. J. J. Clarke and P. W. Trezona, "Towards general systems of colorimetry and photometry based on the tetrachromatic colour match," *Proceedings of the Eighteenth Session of the CIE, London*, 1975, Publ. No. 36 (CIE, Paris, 1976), pp. 205–217.
[5]R. D. Lozano and D. A. Palmer, "The additivity of large-field colour matching functions," Vision Res. 7, 929–937 (1967).
[6]R. D. Lozano and D. A. Palmer, "Large-Field Color Matching and Adaptation," J. Opt. Soc. Am. 58, 1653–1656 (1968).
[7]D. A. Palmer, "Monochromator using graded interference filters," J. Phys. E 4, 41–42 (1971).

Thermal radiation from metal surfaces

A. J. Sievers
Laboratory of Atomic and Solid State Physics and Materials Science Center Cornell University, Ithaca, New York 14853
(Received 17 May 1978)

The thermal radiation from metals is calculated by including the Holstein processes of phonon-assisted and surface-assisted scattering in the free-electron model. This approach provides a fairly accurate description of the experimentally measured total emissivity of good conductors in terms of the dc resistivity and the radius of the free-electron sphere. These calculations do not support the Foote and Davisson–Weeks-type equations which have been used previously.

I. INTRODUCTION

One of the early successes of the Planck radiation law was the apparent agreement between experiment and theoretical calculations of the thermal emissivity of metals. Aschkinass[1] and later Foote[2] calculated the total normal emissivity, ϵ_N of a metal by comparing the spectral emissivity as given by the Hagen-Rubens[3] approximation to that of a black body. Foote found agreement with the measured data on platinum. Foote's equation, which has been slightly modified in the intervening years, is[4]

$$\epsilon_N = 0.578(\rho T)^{1/2} - 0.178(\rho T) + 0.0584(\rho T)^{3/2}, \quad (1)$$

where ρ is the resistivity of the metal in ohm-cm and T is the absolute temperature.

Davisson and Weeks[5] used the Hagen-Rubens relation together with the Fresnel equations to calculate the total hemispherical emissivity ϵ_H of a metal. Their expression, as modified by Parker and Abbott,[6] is

$$\epsilon_H = 0.766(\rho T)^{1/2} - [0.309 - 0.0889\ln(\rho T)]\rho T - 0.0175(\rho T)^{3/2}. \quad (2)$$

Both of these equations have been used extensively in the literature since they relate the total emissivity to one characteristic property of the metal: the dc electrical resistivity.[7,8,9]

In 1965, Parker and Abbott[6] noted that the assumption $\omega\tau \ll 1$ which had been used in the above derivations was not completely valid throughout the frequency region in which thermal radiation was emitted. They calculated the total normal and total hemispherical emissivity by simulating the infrared properties of the metal with a series of exponential functions. For the normal emissivity they found

$$\epsilon_N = 0.578p_1(\rho T)^{1/2} - 0.178p_2(\rho T) + 0.0584p_3(\rho T)^{3/2}, \quad (3)$$

where p_1, p_2, and p_3 were nonlinear functions of the metal relaxation time.

Four different expressions were also obtained for the hemispherical emissivity for four different relaxation times.[6] These expressions for the normal and hemispherical emissivity have not been widely used. The omission comes about not only because these emissivity expressions are specialized, exceedingly intricate, and not amendable to generalization, but also because Parker and Abbott in the same paper showed that the experimental data on a variety of metals both for normal and also hemispherical emissivity followed near universal curves when graphed versus the square root of resistivity times temperature. These universal curves were found to correspond quite closely to those given by Eqs. (1) and (2) above.[6]

In 1977 in a series of papers, Ramanathan and co-workers[10,11,12] reported on the measurement and analysis of the hemispherical emissivity of copper, aluminum and silver. For

 0030-3941/78/6811-1505$00.50

each metal they found the experimentally measured emissivity was much less than predicted in Eq. (2): In addition their relaxation times τ calculated from the Parker and Abbott expressions[6] were up to 45 times smaller than the relaxation times calculated from the dc resistivity.[12] Since the infrared properties of these good conductors are well described by the free-electron-like Drude model[13,14,15] such anomalous behavior for the emissivity is surprising.

In this paper, we re-examine the calculation of the normal and hemispherical emissivity of metals. For the noble metals at elevated temperatures the thermal radiation spectrum occurs almost exclusively in the frequency interval where $\omega\tau > 1$. Previous investigators have always assumed that the thermal radiative properties of the metals were described by $\omega\tau < 1$ in the high-temperature limit. In general, we find that the Hagen-Rubens relation is a poor approximation to use for the metal when calculating the thermal emissivity at room temperature and above. The main purpose of this paper is to develop expressions for the normal and hemispherical emissivities of metals within the limits of the nearly-free-electron model. We obtain simple emissivity equations which depend essentially on two physical characteristics of the metal: the dc resistivity and the free-electron density. When both of these parameters are evaluated by nonoptical means, reasonable agreement between these calculations and published emissivity measurements is found.

In Sec. II, we review the infrared properties of metals. The spectral emissivity is written in terms of the surface resistance of the medium and the Drude model parameters are identified. Both surface scattering and electron-phonon scattering are included. The total emissivities are calculated in Sec. III. We predict that the temperature dependence of the total normal emissivity is proportional to the dc resistivity for a variety of metals (not the square root of the resistivity times temperature). The hemispherical emissivity results are in general more complex but for good conductors, such as the noble metals, the temperature dependence is again proportional to the dc resistivity. In Sec. IV, we show how contributions from other absorption processes such as interband transitions and electron-electron scattering may produce characteristic temperature dependences in the total emissivity of a metal.

II. IR PROPERTIES OF METALS

To calculate the thermal emissivity of metals we need to know the absorptivity of metals in the blackbody spectral region. By Kirchoff's law this spectral absorptivity at a given temperature is equal to the spectral emissivity at the same temperature.[4] This spectral emissivity is folded together with the black-body spectrum to find the total emissivity.

The radiant spectral power emitted by a surface element of a black body in a given direction per unit frequency interval per unit solid angle is given by Planck's law

$$L_\omega = \frac{1}{\pi}\left(\frac{1}{2\pi c}\right)^2 \frac{\hbar\omega^3}{\exp(\hbar\omega/kT) - 1}, \tag{4}$$

where ω is the angular frequency, c is the velocity of light in vacuum, $\hbar$ is Planck's constant divided by 2π and k is Boltzmann's constant.

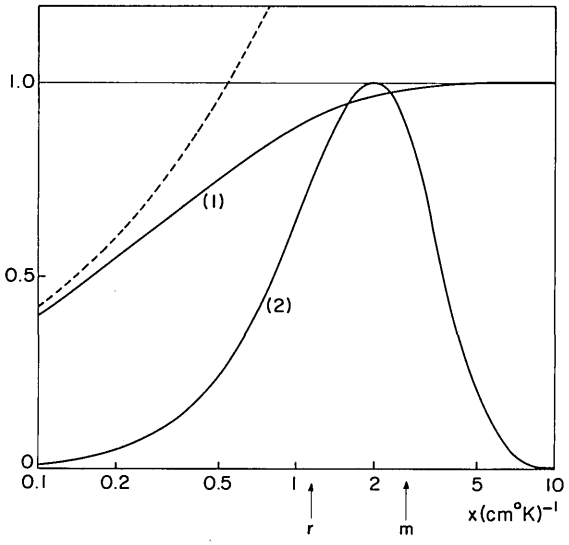

FIG. 1. Normalized black body and metal absorptivity functions used in the text. Curve 2 gives the normalized spectral distribution of the black body where m is the centroid value. The normalized spectral distribution of $g(x,r)$ for a particular value of $r(=1.14)$ is given by curve 1. The dashed line gives the Hagen-Rubens result for the same relaxation frequency. $r = 1.14$ is the correct value for Cu when the scattering contributions described in Secs. III C and III D are included.

A characteristic frequency of this black-body spectrum which is useful in analyzing the emissivity problem is the centroid frequency $\langle\omega\rangle$ where

$$\langle\omega\rangle = \int_0^\infty \omega L_\omega \, d\omega \Big/ \int_0^\infty L_\omega \, d\omega. \tag{5}$$

It is convenient to normalize frequency with respect to temperature so we define new variables

$$x = \tilde{\nu}/T \quad \text{and} \quad m = (\langle\tilde{\nu}\rangle/T)\ (\text{cm °K})^{-1}, \tag{6}$$

where $\omega = 2\pi c\tilde{\nu}$ and $\tilde{\nu}$ is the frequency measured in cm^{-1}. We find, using Eqs. (5) and (6),

$$\langle\tilde{\nu}\rangle = 2.665T\ \text{cm}^{-1}. \tag{7}$$

The centroid of a room temperature black-body spectrum is at 800 cm^{-1}. The normalized spectral distribution of the black-body spectrum is given by curve 2 in Fig. 1. Most of the spectral weight associated with curve 2 comes from a decade of x values centered around m. The scaling of all frequencies with temperature dictates that the infrared properties of metals, not the far infrared or optical properties, will play the dominant role in determining the high-temperature emissivities of metals.

A. Surface impedance

The concept of surface impedance is often used to describe the interaction of electromagnetic radiation with a metal when the frequency of the radiation is much less than the plasma frequency.[16] The usual definition of surface impedance ignores the displacement current and uses only the conduction current. At normal incidence $Z(\omega)$ is defined as

$$Z(\omega) = R(\omega) + iX(\omega) = E_0 \Big/ \int_0^\infty j(z)\, dz, \tag{8}$$

where E_0 is the parallel component of the electric field at the

metal surface (which is perpendicular to the z axis) and $j(z)$ is the current density at a depth z beneath the surface.

The electromagnetic fields within a metal are described by Maxwell's equations together with an equation relating the electric field and the current density. For cases in which the electromagnetic field skin depth ($= \delta$), does not vary appreciably over the range of an electron mean free path ($l = v_F\tau$), or the distance an electron travels during one radian of the radiation (v_F/ω), a local conductivity $\sigma(\omega)$ can be defined where

$$j(z,\omega) = \sigma(\omega)E(z,\omega)$$

and $j(z,\omega)$ *and* $E(z,\omega)$ are the current density and electric field at the position z and the frequency ω. Frequently for pure metals $\delta \ll l$ and $\delta \ll v_F/\omega$ (anomalous skin effect) or that $v_F/\omega \ll \delta \ll l$ (surface scattering effect) and a nonlocal relationship between the current density and electric field must be used. Very complicated wave forms occur for the fields inside the metal. The surface impedance concept permits a reformulation of the problem in terms of a boundary condition on the fields at the metal surface.

The boundary condition is easily obtained from Maxwell's equations and the definition of surface impedance. Because of the rapid attenuation of the fields within the metal it is necessary to retain only the derivatives normal to the surface in Maxwell's equations. With this restriction the fields are tangential to the metal surface. Integrating the induction equation we find

$$\vec{E}_t(0) = (Z/Z_0)\vec{H}_t(0) \times \hat{n}, \tag{9}$$

where the subscript t signifies tangential fields, Z_0 is the impedance of free space, and n is the normal to the metal. The coefficient Z/Z_0 in Eq. (9) is the only quantity characterizing the metal which must be known in order to find the external electromagnetic field. This boundary condition is valid even though the field inside the metal may not be described by the usual macroscopic Maxwell's equations.[17] This surface impedance concept should be contrasted with the corresponding description of the absorptivity of a metal in terms of a complex index of refraction. This latter description is only reasonable when the fields are attenuated exponentially within the metal.[18]

The reflectivity ρ and absorptivity α of electromagnetic radiation normally incident on a metal surface with surface impedance Z are given by

$$\rho = \left|\frac{1 - Z/Z_0}{1 + Z/Z_0}\right|^2 \tag{10}$$

and

$$\alpha = 1 - \rho = \frac{4(R/Z_0)}{[1 + (R/Z_0)]^2 + (X/Z_0)^2}. \tag{11}$$

For most metals R/Z_0, $X/Z_0 \ll 1$ so that the absorptivity reduces to

$$\alpha \simeq 4\,R/Z_0, \tag{12}$$

which by Kirchhoff's law is the spectral emissivity.[4]

B. Classical skin effect limit

In this domain the electron mean free path is much less than the skin depth so the conductivity can be treated as local. The Drude model conductivity is

$$\sigma(\omega) = \sigma_1 + i\sigma_2 = \frac{\sigma_0}{1 + i\omega\tau}, \tag{13}$$

where $\sigma_0 = \omega_p^2\tau/4\pi$ and τ is the relaxation time. The corresponding surface impedance is

$$Z(\omega)/Z_0 = (1 + i)[(\omega/2\omega_p)(1/\omega_p\tau)]^{1/2}(1 + i\omega\tau)^{1/2} \tag{14}$$

so that

$$R/Z_0 = (1/2\omega_p\tau)(2\omega\tau)^{1/2}[(1 + \omega^2\tau^2)^{1/2} - \omega\tau]^{1/2} \tag{15}$$

and

$$X/Z_0 = (1/2\omega_p\tau)(2\omega\tau)^{1/2}[(1 + \omega^2\tau^2)^{1/2} + \omega\tau]^{1/2}. \tag{16}$$

By Eq. (12) the absorptivity is directly related to the real part of the surface impedance and hence

$$\alpha = (2/\omega_p\tau)(2\omega\tau)^{1/2}[(1 + \omega^2\tau^2)^{1/2} - \omega\tau]^{1/2}. \tag{17}$$

In the nonrelaxation region where $\omega\tau \ll 1$ the absorptivity is

$$\alpha = (2/\omega_p\tau)(2\omega\tau)^{1/2} \tag{18}$$

which is the Hagen-Rubens result.

In the extreme relaxation region where $\omega\tau \gg 1$ the absorptivity is

$$\alpha = 2/\omega_p\tau, \tag{19}$$

which is the Mott-Zener result.

For copper at room temperature $\langle\omega\rangle\tau = 3.7$ and the infrared spectral absorptivity and emissivity are characterized to a first approximation by Eq. (19). At high temperatures the resistivity of pure metals is dominated by electron-phonon scattering.[19] For temperatures large compared to the characteristic Debye temperature, Θ, of the solid the number of phonon scatters is proportional to T, so

$$1/\tau \sim T \quad \text{for} \quad T > (2/3)\Theta. \tag{20}$$

Since $\langle\omega\rangle$ is proportional to T and τ is inversely proportional to T then to a good approximation $\langle\omega\rangle\tau = 3.7$ for copper at all temperatures.

To take advantage of this temperature-invariant behavior, we normalize the relaxation frequency by temperature in the same manner as was done for the black-body frequencies [Eq. (6)].

The normalized relaxation frequency r of the metal is

$$r = (2\pi c\tau T)^{-1}\ (\text{cm}\ ^\circ\text{K})^{-1}. \tag{21}$$

Combining Eqs. (6) and (21), $m/r = 3.7$ for copper.

For metals which are not characterized by the extreme relaxation region the general expression given by Eq. (17) must be used to calculate the spectral emissivity. Substituting Eq. (21) into Eq. (17) we find

$$\epsilon = \frac{2}{\omega_p\tau}\left(2\frac{x}{r}\right)^{1/2}\left\{\left[1 + \left(\frac{x}{r}\right)^2\right]^{1/2} - \frac{x}{r}\right\}^{1/2} \tag{22}$$

or

$$\epsilon = (2/\omega_p\tau)g(x,r), \tag{23}$$

where so far r is independent of frequency and temperature.

The normalized frequency dependence of $g(x,r)$ in Eq. (23) for a particular r ($r = 1.14$) is represented by curve 1 in Fig. 1. The dashed line gives the Hagen-Rubens result for the same relaxation frequency. From the dc resistivity the normalized relaxation frequency for Cu is $r = 0.72$. To represent this metal curve 1 in Fig. 1 should be translated to the left from $r = 1.14$ to 0.72. The relative position of this curve with respect to the black-body curve is determined simply by the position of the relaxation frequency r with respect to the black-body centroid frequency m.

At high temperatures r is not strictly temperature independent for most metals. For Cu, Ag, Au, and Al, r increases slightly with increasing temperature. This is due mainly to thermal expansion and the consequent decrease in the Debye temperature Θ. For the free-electron model[20] $r\alpha(1/\Theta)^2$ so

$$d/dT(\ln r) = 6a\gamma, \tag{24}$$

where a is the linear thermal expansion coefficient and γ is the Grüneisen constant. For values of T not too large this equation integrates to

$$r(T) = \text{const}(1 + 6a\gamma T). \tag{25}$$

This formula can be used to compare the relaxation parameter at any two temperatures.

Unfortunately this simple expression for r does not work for other metals such as Pt, Pd, and Ta. For these metals r decreases with increasing temperature. At the present time it is not possible to predict the exact temperature dependence of r for the different metals so we must determine r at each temperature from the dc resistivity and r_s, the radius of the free-electron sphere, a quantity which is a measure of the electron density. They are related by[21]

$$\frac{1}{\tau} = \frac{4.545 \times 10^{14}\, \rho_\mu(T)}{(r_s/a_0)^3}\ (\text{s}^{-1}),$$

so

$$r(T) = \frac{2411}{(r_s/a_0)^3}\frac{\rho_\mu(T)}{T}, \tag{26}$$

where $\rho_\mu(T)$ is the dc resistivity measured in $\mu\Omega$ cm and a_0 is the Bohr radius. Values of r_s at room temperature have been tabulated for most metals.[21,22] The temperature dependence of r_s is determined by the thermal expansion of the lattice so

$$\frac{d}{dT}[\ln(r_s/a_0)^3] = \frac{d}{dT}(\ln V) = 3a. \tag{27}$$

Since the changes in $(r_s/a_0)^3$ with temperature are typically less than 2%, we shall neglect this temperature dependence and use the room-temperature values of r_s throughout this paper. We complete our identification of the spectral emissivity for the Drude model by noting that

$$2/\omega_p\tau = 5.263 \times 10^{-6}\,(r_s/a_0)^{3/2} T\, r(T). \tag{28}$$

For good metals where $r < m$ it is apparent from Fig. 1 that the spectral emissivity in the black-body decade is frequency independent. In this limit the total normal emissivity ϵ_N becomes

$$\epsilon_N = \frac{1.269 \times 10^{-2}\, \rho_\mu(T)}{(r_s/a_0)^{3/2}}, \quad r < m \tag{29}$$

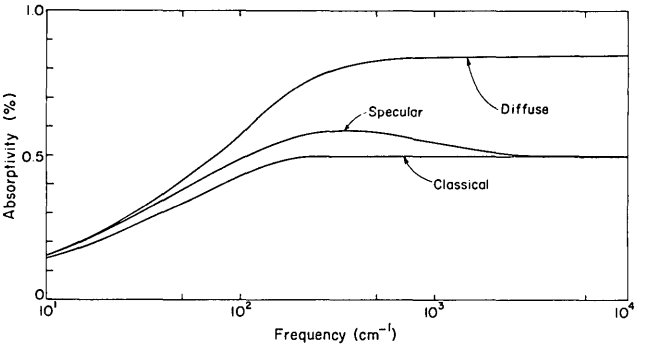

FIG. 2. The absorptivity of copper near room temperature. Dingle's tables (Ref. 25) have been used to estimate the diffuse and specular surface scattering limits. The classical skin effect is also shown for comparison.

and the emissivity is proportional to the dc resistivity. Equation (29) was derived in the same limit as and should be compared with Eq. (1). For good conductors with $\rho \sim T$ both equations predict a linear temperature dependence of the total normal emissivity. [Note that ρ in Eq. (1) is given in Ω cm]. The main difference between the two equations is that the coefficient of Eq. (1) is much larger than that of Eq. (29) [for copper (Eq. 1) $\approx$ 2.6 (Eq. 29)]. But Eq. (29) represents an upper limit to the spectral emissivity since it corresponds to replacing curve 1 in Fig. 1 by the value 1 for all x. We conclude that Eq. (1) is a poor approximation for good conductors. We now go on to consider other absorption processes which are known to contribute to the infrared absorptivity of metals but which have not been included in earlier derivations of the total emissivities.

C. Surface scattering

The infrared properties of metals have been analyzed in some detail by Reuter and Sondheimer,[23] Holstein,[24] Dingle,[25] and Pippard,[26] and others.[14,15] The predicted infrared absorption is quite different depending on whether the conduction electrons colliding with the metal surface are specularly reflected or are diffusely reflected. The final expressions for the electric and magnetic fields involve complicated integrals which Dingle has computed and tabulated for a variety of cases. In Fig. 2 we present the absorptivity of copper near room temperature as obtained from Dingle's tables.[25] Note that the diffuse absorptivity is always larger than the specular absorptivity. Also plotted is the predicted infrared absorption associated with the classical theory which we reviewed in Sec. I. It is clear that the classical theory is in poor agreement with the more complete Dingle results. The physical reason for this difference is that the classical theory does not take appropriate account of the surface. It is easiest to understand the surface absorption by focusing our attention on the region of interest, namely the high-frequency relaxation region where $\omega\tau > 1$. From Eq. (19) the absorptivity is

$$\alpha = 2/\omega_p\tau_e, \tag{30}$$

where τ_e is now an effective relaxation time. We next assume that the electrons scatter diffusely from the surface but do not scatter in the bulk so that there is one collision in the time needed to cross the electromagnetic skin depth ($\delta = c/\omega_p$) to the surface and back again. Thus

$$\tau_e \simeq \frac{2c/\omega_p}{v_F},$$

so

$$\alpha_s \simeq v_F/c. \tag{31}$$

A more accurate calculation of the absorptivity associated with diffuse surface scattering gives[24,25]

$$\alpha_s = (3/4)(v_F/c). \tag{32}$$

We next include bulk scattering by assuming that the bulk- and surface-scattering mechanisms are independent. The effective relaxation time becomes

$$\frac{1}{\tau_e} = \sum_i \frac{1}{\tau_i}, \tag{33}$$

$$1/\tau_e = (1/\tau_b) + (3/8)(\omega_p/c)\, v_F. \tag{34}$$

In the region where $\omega\tau > 1$ Eqs. (34) and (30) give absorptivities for copper which are slightly larger than Dingle's exact results.

The calculated absorptivity for the specular reflection case with copper is also shown in Fig. 2. The absorptivity associated with specular reflection actually passes through a maximum at low frequencies.[26] This low-frequency anomalous skin-effect absorption is not a surface absorption (in the sense of the one described above). When the radiation frequency $\omega < (\vec{k}\cdot\vec{v}_F)$ where $\vec{k}$ is the wave vector of the radiation and $\vec{v}_F$ the Fermi velocity vector, the electrons can absorb a photon directly and conserve both energy and momentum. In fact, the effective electrons for this process are those which do not hit the surface but "surfride" with the electromagnetic field through the skin depth. This anomalous skin-effect absorption is relatively insensitive to boundary conditions (in contrast to the higher-frequency case treated earlier) and it is not obvious that the absorption mechanisms are additive in this low-frequency region. At low temperatures and low frequencies the electrodynamic properties of the metal approach those characterized by the extreme anomalous limit where $v_F\tau/\delta \gg 1$ and $v_F\tau/\delta \gg (1+\omega^2\tau^2)^{3/2}$. The absorptivity is

$$\alpha_\infty = [(4\sqrt{3}/\pi)(v_F/c)]^{1/3}(\omega/\omega_p)^{2/3} \tag{35}$$

which is independent of the relaxation time. This expression is essentially independent of the diffuse- or specular-scattering boundary conditions since specular is 8/9 ths of diffuse. Fortunately, as we now show, this low-frequency anomalous skin-effect region does not play an important role in the high-temperature emissivity determination.

The results discussed above can be summarized with a frequency-relaxation time diagram which identifies the four different kinds of regions which we have specified.[27,28] Such a diagram is given for copper in Fig. 3: region C is the transmission region where $\omega > \omega_p$; region (A) is the classical skin effect where $v_F\tau \ll \delta$ and $\omega\tau \ll 1$; region (B) is the classical relaxation region where $v_F\tau \ll \delta$ and $\omega\tau \gg 1$; region (D) the anomalous skin effect where $\delta \ll v_F\tau$ and $\delta \ll v_F/\omega$ and region (E) the surface scattering effect where $v_F/\omega \ll \delta \ll v_F\tau$. For copper at room temperature $\langle\omega\rangle\tau > 1$ and $v_F/\langle\omega\rangle = 100$ Å $< \delta = 180$ Å $< v_F\tau = 210$ Å. The cross-hatched parallelogram in Fig. 3 indicates the area of the frequency-relaxation time plane which contributes to the thermal emissivity of copper at elevated temperatures. A given horizontal line identifies the dc relaxation time at a particular temperature while the length of the line defines the most effective decade of thermal frequencies in the black-body spectrum. Good conductors described by different dc relaxation times can be simulated to some extent by a vertical shift of the parallelogram in Fig. 3 to the new relaxation time.[29] This diagram demonstrates that the relaxation region (B) and the surface scattering region (E) of copper completely determine the amount of thermal radiation emitted. For metals with shorter relaxation times the normal skin-effect region (A) will play a secondary role. In all cases for $T > \Theta$ the anomalous skin effect (D) can be neglected.

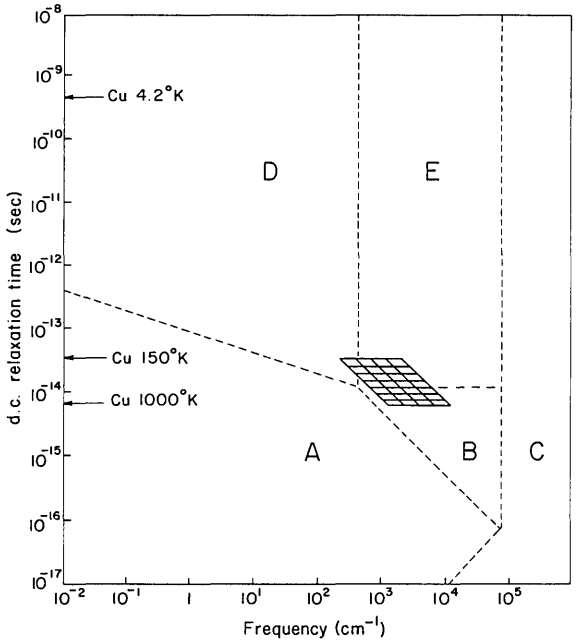

FIG. 3. Frequency-relaxation time diagram for copper. Region (*A*) is the classical skin effect where $v_F\tau \ll \delta$ and $\omega\tau \ll 1$; region (*B*) is the classical skin effect where $v_F\tau \ll \delta$ and $\omega\tau \gg 1$; region (*D*) the anomalous skin effect where $\delta \ll v_F\tau$ and $\delta \ll v_F/\omega$ and region (*E*) the surface scattering effect where $v_F/\omega \ll \delta \ll v_F\tau$. The metal becomes transparent in region *C*. (After Refs. 27 and 28). The cross hatched parallelogram indicates the important region for the thermal emissivity of copper at high temperatures.

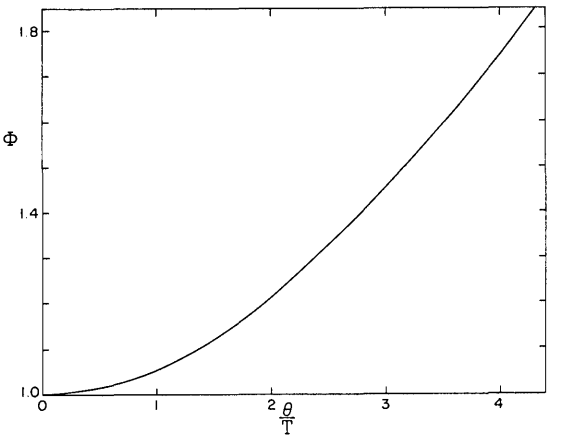

FIG. 4. Temperature-dependent correction factor for the dc electron-phonon scattering time. The Debye temperature is Θ.

D. Electron-phonon scattering

Holstein has demonstrated that another relaxation mechanism which is purely a bulk process has been neglected in the classical theory.[30] He showed that at 0 °K there is bulk absorption due to phonon generation by the excited electrons. Gurzhi[31] has given an explicit formula for this quantum effect which relates the effective τ_H which includes the Holstein effect to the dc relaxation time τ_b obtained from the dc resistivity,

$$1/\tau_H = \Phi(T)\, 1/\tau_b, \tag{36}$$

where

$$\Phi(T) = \frac{2}{5}\frac{\theta}{T} + 4\left(\frac{T}{\theta}\right)^4 \int_0^{\theta/T} \frac{v^4\, dv}{e^v - 1}. \tag{37}$$

$\Phi(T)$ is plotted versus θ/T in Fig. 4. Note that for temperatures $T > \theta$, $\Phi(T)$ differs from 1 by less than 5%. Our final expression for the relaxation time in the diffuse scattering limit is

$$1/\tau_e = \Phi(T)/\tau_b + (3/8)(\omega_p/c)v_F. \tag{38}$$

The corresponding normalized relaxation frequency is

$$r(T) = \frac{2411}{(r_s/a_0)^3}\frac{\rho_\mu(T)}{T}\Phi(T) + \frac{1995}{(r_s/a_0)^{5/2}T}. \tag{39}$$

A comparison of Eq. (39) with Eq. (26) indicates that the diffuse surface scattering term introduces a temperature dependence to the characteristic relaxation frequency of the metal. In general, r at high T will be smaller than r at room temperature so that if a metal satisfies the condition $m/r > 1$ ($\langle\omega\rangle\tau > 1$) at room temperature then it is surely satisfied at elevated temperatures.

Equations (39), (28), and (23) define the spectral emissivity of metals in the infrared. This emissivity depends mainly on two physical quantities, ρ_μ and r_s. The third parameter Θ which determines $\Phi(T)$ plays a secondary role at room temperature. At high temperatures where $\Theta/T < 1$, $\Phi(T) \simeq 1$ and the temperature dependence associated with the Holstein effect can be ignored. In any event all three of these parameters are obtained from other than optical measurements.

III. TOTAL EMISSIVITIES FOR FREE ELECTRON METALS

A. Total normal emissivity

The total normal emissivity is defined by the equation

$$\epsilon_N = \int_0^\infty \epsilon L_\omega\, d\omega \Big/ \int_0^\infty L_\omega\, d\omega, \tag{40}$$

where L_ω is given by Eq. (4) and ϵ by Eq. (11). In general this integral is a function of ω_p, v_F, and τ (or in our notation r_s and ρ_μ). But since R/Z_0, $X/Z_0 \ll 1$ for most metals, it is useful to introduce another integral η which approaches ϵ_N in this limit. We set

$$\eta = \int_0^\infty \frac{4R}{Z_0} L_\omega\, d\omega \Big/ \int_0^\infty L_\omega\, d\omega. \tag{41}$$

Subsitituting Eq. (23) the integral can be rewritten as

$$\eta = (2/\omega_p\tau)g_1(r) \tag{42}$$

where

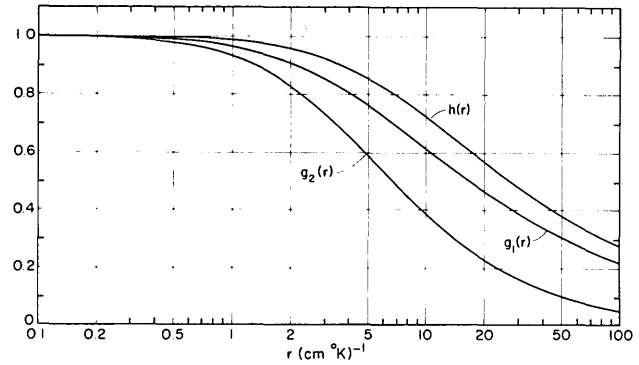

FIG. 5. The relaxation frequency dependence of three overlap integrals used in the text. These integrals are tabulated in Appendix I.

$$g_1(r) = \int_0^\infty g(x,r)L_x\, dx \Big/ \int_0^\infty L_x\, dx$$

describes the spectral overlap between the two functions.

$2/\omega_p\tau$ and r are given in terms of ρ_μ and r_s by Eqs. (28) and (39), respectively. The function $g_1(r)$ is graphed in Fig. (5) and tabulated in Appendix I. Inspection of Fig. 5 shows that for $r < 2$ then $g_1(r)$ differs from 1 by 10% or less. For good conductors it is a reasonable approximation to set $g_1(r) \approx 1$. In addition for $T > \Theta$ then $\Phi(T) = 1$ so Eq. (42) reduces to

$$\eta \approx \frac{1.269 \times 10^{-2}}{(r_s/a_0)^{3/2}}\rho_\mu(T) + \frac{1.050 \times 10^{-2}}{(r_s/a_0)}, \quad \begin{pmatrix} r < 2 \\ T > \Theta \end{pmatrix}. \tag{43}$$

Also in this limit $\eta \approx \epsilon_N$ so the temperature dependence of ϵ_N is given by the temperature dependence of the dc resistivity.

When $r \gg 2$ then $r(T)$ must be found at each temperature from $\rho_\mu(T)$ as given by Eq. (39) and then $g_1(r)$ determined. Typical curves for r vs T for different elements[32] are shown in Fig. 6. For a given element r varies by as much as 30% from the room-temperature values. However, since $g_1(r)$ is a slowly varying function of r [in the region of largest variation a 20% change in r produces a 5% change in $g_1(r)$] $g_1(r)$ can be eval-

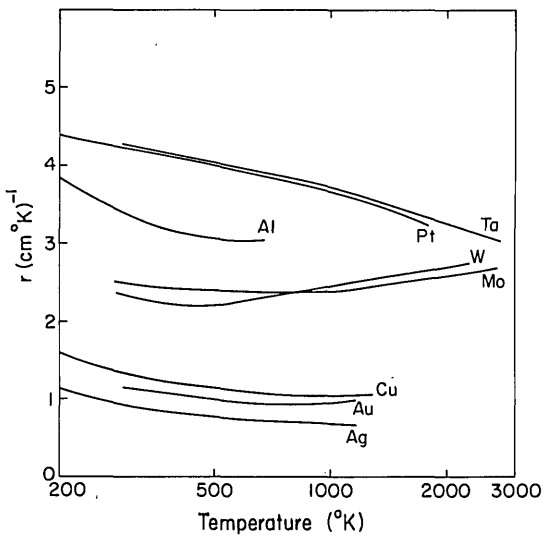

FIG. 6. The temperature dependence of the relaxation frequency for different elements. These r's are calculated from Eq. (39) in the text.

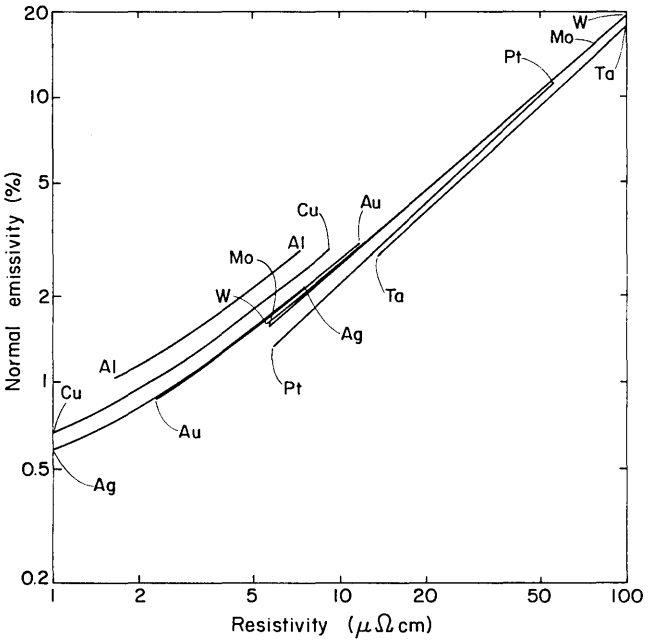

FIG. 7. The total normal emissivity as a function of resistivity for a number of elements. These curves are calculated from Eq. 40 in the text. Since this calculation only counts the conduction electron contribution to the emissivity, these curves define lower bounds for real metals.

uated once at the middle of the temperature range of interest and treated as a constant. With $g_1(r)$ constant once again the temperature dependence of ϵ_N is given by the temperature dependence of the dc resistivity.

Although we shall not attempt to calculate the low-temperature emissivity it is perhaps worth noting that another simple case occurs at extremely low temperatures, $T \ll \Theta$, when $r \to 0$. In this extreme anomalous skin-effect limit the spectral emissivity is given by Eq. (35) and the total emissivity becomes

$$\epsilon_N = 1.10 \times 10^{-4} (r_s/a_0)^{2/3} T^{2/3}, \quad (T \ll \Theta, r \to 0) \quad (44)$$

The emissivity is simply related to the electron density.

We have computed the total emissivity ϵ_N given by the general expression in Eq. (40) and plotted these results versus dc resistivity in Fig. 7. For metals which have resistivities less than 10 $\mu\Omega$ cm surface scattering plays an important role in determining the emissivity while for metals with larger dc resistivities the nearly linear slope in Fig. 7 indicates that ϵ_N is determined essentially by the dc resistivity. The vertical mismatch between elements gives a measure of the importance of r_s in the emissivity determination.

We have also compared these results for ϵ_N to those given by the simpler expression (Eq. 42) which relates ϵ_N to η when $r < m$. The ratio of these two quantities is plotted versus resistivity at the bottom of Fig. 8. Only one average curve is shown since the curves for the different elements are very close to each other. For $\rho_\mu < 10$ $\mu\Omega$ cm, less than a 1% error is introduced by using the value given by η for the emissivity while for ρ_μ between 10 and 100 $\mu\Omega$ cm the difference ranges from 1% to 12%.

The experimental and calculated values of ϵ_N for Pt are compared in Fig. 9. Curve A shows ϵ_N as measured by Abbott.[33] ϵ_N as calculated from Eq. (1) and as calculated from Eq. (40) are also shown. Since Eq. (1) resulted from taking the Hagen-Rubens limit ($\omega\tau \ll 1$) of the Drude model while Eq. (40) makes no such approximation and is exact for the Drude model, the good agreement between Foote's equation [Eq. (1)] and Curve A is simply fortuitous. The curve from Eq. (40), on the other hand, identifies the minimum ϵ_N possible for Pt since only the free-electron contribution has been counted. Contributions to the infrared properties from other electrons (interband transitions) can only increase the value of ϵ_N over that given in Fig. 9. These contributions will be discussed in Sec. IV.

Since Ta has a relaxation frequency very similar to that for Pt (Fig. 6) we compare calculations and experiments on this

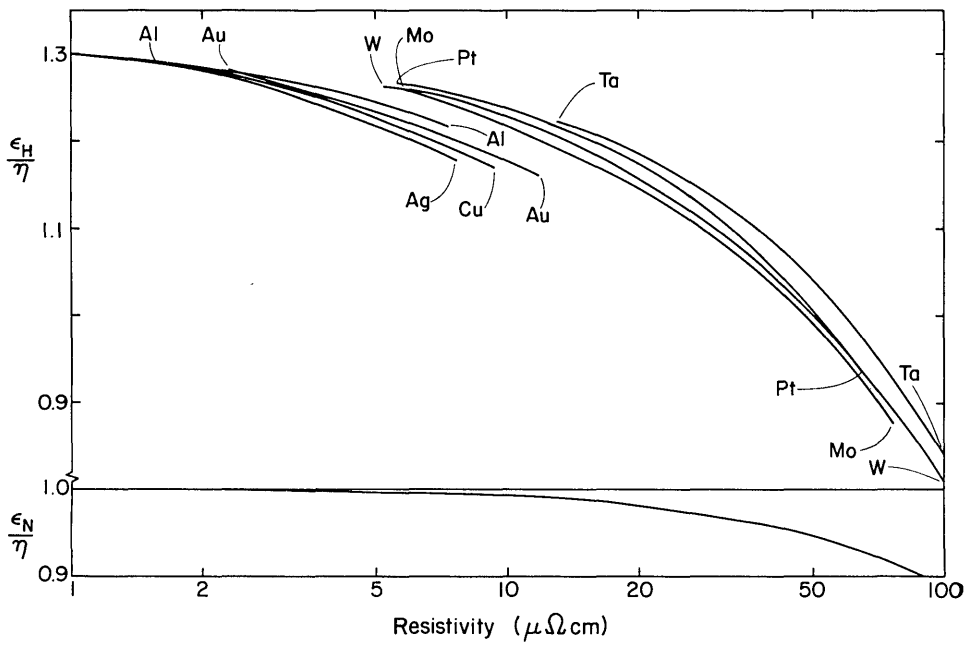

FIG. 8. Two emissivity ratios vs dc resistivity. ϵ_N is calculated with Eq. (40) while η is calculated with Eq. (42), ϵ_H is calculated with Eq. (45).

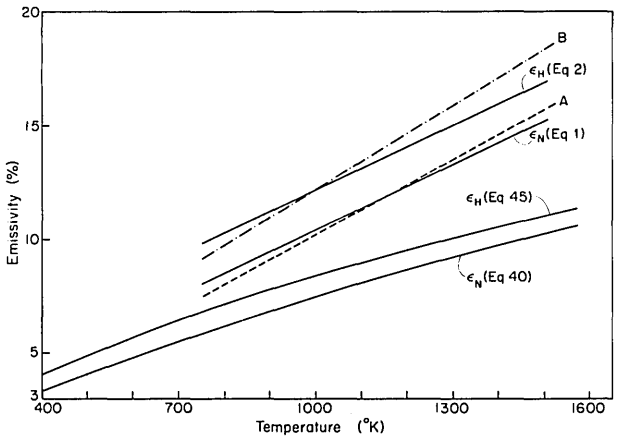

FIG. 9. Experimental and calculated values for the emissivities of Pt vs temperature. The dashed curve *A* shows the experimental values obtained by Abbott (Ref. 33) for ϵ_N. These results are compared with the approximate Foote calculation [Eq. (1)] and with the exact calculation in the text [Eq. (40)]. The dot-dashed curve *B* shows the experimental data for ϵ_H vs temperature. These results are to be compared with the Davisson-Weeks calculation [Eq. (2)] and with the exact calculation described in the text [Eq. (45)]. Since Eq. (1) and Eq. (2) represent approximate solutions to Eq. (40) and Eq. (45), the good agreement between these solutions and the experimental data is fortuitous.

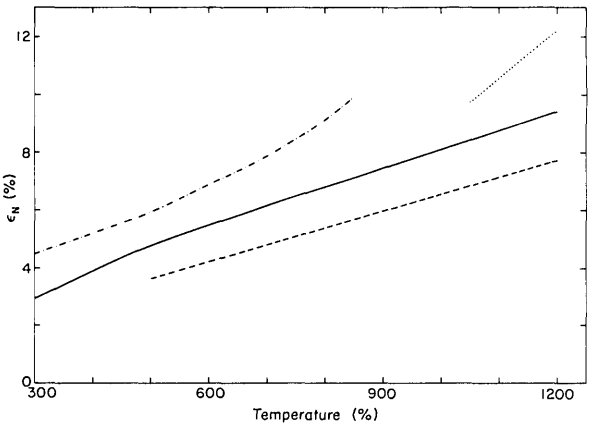

FIG. 10. Experimental and calculated values for the emissivities of Ta vs temperature. The dot-dash curve shows the data of Blickensderfer *et al.* (Ref. 34); the dotted curve, the data of Zhorov (Ref. 35) and the dashed curve, the data of Betz *et al.* (Ref. 36). The solid line represents the calculated values of ϵ_N given by Eq. (40).

metal in Fig. 10. The experimental data of Blickensderfer *et al.*,[34] Zhorov,[35] and Betz *et al.*[36] show quite a spread. Betz's data (dashed curve) in particular is below ϵ_N as given by Eq. (40). Since this calculated curve is expected to identify the minimum possible ϵ_N, either the r_s we used is wrong[22] or the data are in error.

B. Total hemispherical emissivity

The total hemispherical emissivity of a metal is defined as the total power radiated by the metal into a hemisphere compared to the total power radiated by a black body into the same solid angle so[4]

$$\epsilon_H = \int_0^\infty \int_0^{\pi/2} \epsilon(\theta) L_\omega d(\sin^2\theta)\, d\omega \Big/ \int_0^\infty L_\omega\, d\omega, \quad (45)$$

where θ is the polar angle measured with respect to the metal normal and

$$\epsilon(\theta) = \tfrac{1}{2}[\epsilon_{TM}(\theta) + \epsilon_{TE}(\theta)] \quad (46)$$

is the emissivity for unpolarized radiation. $\epsilon_{TM}(\theta)$ is the emissivity for plane polarized radiation with the plane of polarization parallel to the plane of incidence (transverse magnetic) and $\epsilon_{TE}(\theta)$ is the emissivity for plane polarized radiation with the plane of polarization normal to the plane of incidence (transverse electric). The angular dependence of the emissivities is obtained from the Fresnel equations.[17,37] We find for metals where R/Z_0, $X/Z_0 \ll 1$ that

$$\epsilon_{TM}(\theta) = \frac{(4R/Z_0)\cos\theta}{\cos^2\theta + (2R/Z_0)\cos\theta + (R^2+X^2)/Z_0^2} \quad (47)$$

and

$$\epsilon_{TE}(\theta) = \frac{(4R/Z_0)\cos\theta}{1 + (2R/Z_0)\cos\theta}. \quad (48)$$

The angular dependence of emissivity for *TM* waves has a maximum at $\theta_m = \cos^{-1}(2R/Z_0)$ while the angular dependence of emissivity for *TE* waves has essentially a simple cosine dependence. Because of the different angular dependences we calculate the contribution of the *TM* and *TE* waves to the total emissivity separately.

We find that

$$\frac{\epsilon_{TM}}{2} = \frac{\int_0^\infty \frac{4R}{Z_0}\left(1 + \frac{R}{Z_0}\left\{\left(\frac{1}{\zeta} - \zeta\right)\left[\tan^{-1}\left(\frac{1+R}{\zeta R}\right) - \tan^{-1}\left(\frac{1}{\zeta}\right)\right] + \ln\left(\frac{R^2}{Z_0^2}\cdot\frac{1+\zeta^2}{1+2R/Z_0}\right)\right\}\right) L_x\, dx}{\int_0^\infty L_x\, dx} \quad (49)$$

where

$$\zeta^2 = \frac{[[1 + (x/r)^2]^{1/2} + x/r]}{[(1 + (x/r)^2)^{1/2} - x/r]},$$

and

$$\frac{\epsilon_{TE}}{2} = \frac{\int_0^\infty \frac{4R}{3Z_0}\left(1 - \frac{3}{8}\left(\frac{4R}{Z_0}\right) + \frac{3}{20}\left(\frac{4R}{Z_0}\right)^2 - \cdots\right) L_x\, dx}{\int_0^\infty L_x\, dx}. \quad (50)$$

Both of these expressions simplify in the limit $r < m$ to

$$\epsilon_{TM}/2 \rightarrow \eta \tag{51}$$

and

$$\epsilon_{TE}/2 \rightarrow \eta/3, \tag{52}$$

where η is given by Eq. (42). For good conductors the hemispherical and normal emissivities are simply related. Combining Eq. (51) and (52) we have

$$\epsilon_H = (4/3)\,\epsilon_N, \quad (r < m). \tag{53}$$

For large values of r the simplification of Eq. (49) is not so obvious. The frequency dependences of the different terms in Eq. (49) are such that a near cancellation of some of the terms results. With a 10% loss in accuracy we can replace Eq. (49) by

$$\frac{\epsilon_{TM}}{2} = \frac{\int_0^\infty \frac{4R}{Z_0}\left[1 + \frac{2R}{Z_0}\ln\left(\frac{R}{Z_0}\right)\right] L_x\, dx}{\int_0^\infty L_x\, dx}. \tag{54}$$

Neglecting the frequency dependence of the ln term we find

$$\frac{\epsilon_{TM}}{2} \approx \frac{2}{\omega_p\tau}\left(g_1(r) - \frac{1}{\omega_p\tau} g_2(r)\ln(\omega_p\tau)\right), \tag{55}$$

where $g_1(r)$ is defined by Eq. (42) and

$$g_2(r) = \int_0^\infty g^2(x,r) L_x\, dx \Big/ \int_0^\infty L_x\, dx.$$

$g_2(r)$ is graphed in Fig. 5 and tabulated in Appendix I. Note that $g_2(r) \approx g_1^2(r)$.

In a similar manner Eq. (50) integrates to

$$\frac{\epsilon_{TE}}{2} \approx \frac{2}{3\omega_p\tau}\left(g_1(r) - \frac{3}{4\omega_p\tau} g_2(r)\right). \tag{56}$$

Together Eqs. (55) and (56) give a good approximation to the hemispherical emissivity which is

$$\epsilon_H \approx (8/3)[g_1(r)/\omega_p\tau] - [g_2(r)/(\omega_p\tau)^2](\tfrac{1}{2} + 2\ln\omega_p\tau). \tag{57}$$

Again $2/\omega_p\tau$ and r are given in terms of ρ_μ and r_s by Eqs. (28) and (39), respectively.

At low temperatures in the extreme anomalous limit the hemispherical emissivity which corresponds to Eq. (44) is

$$\epsilon_H = 1.46 \times 10^{-4}\,(r_s/a_0)^{2/3} T^{2/3}, \quad (T \ll \Theta, r \rightarrow 0). \tag{58}$$

With Eqs. (49) and (50) we have also computed ϵ_H/η as a function of dc resistivity for a variety of metals. The results are shown in the top part of Fig. 8. For $\rho_\mu < 10\ \mu\Omega$ cm, ϵ_H can be set equal to $(4/3)\epsilon_N$ with less than a 10% error. For $\rho_\mu > 10\ \mu\Omega$ cm a simple dependence on η does not occur [but see Eq. (57)]. The anomalous behavior comes about because the angle of maximum absorption for the *TM* waves also depends on the dc resistivity of the material. It is this dependence which produces the rapid variation in ϵ_H/η with dc resistivity.

In Fig. 11 the hemispherical emissivity for the same group of metals is plotted versus resistivity. Although the hemispherical emissivity does not vary as the first power of resistivity, a near universal dependence is still observed.

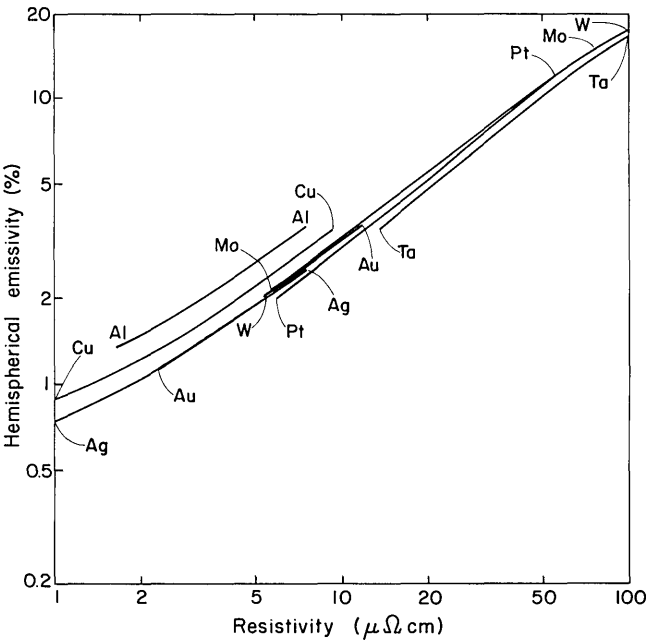

FIG. 11. The total hemispherical emissivity as a function of dc resistivity for a number of elements. These curves are calculated from Eq. (45) in the text. Since this calculation only counts the conduction electron contribution to the emissivity, these curves define lower bounds for real metals.

Experimental and calculated values of ϵ_H for Pt are compared in Fig. 9. Curve *B* shows ϵ_H as measured by Abbott.[33] These results should be compared with the calculated values given by Eqs. (2) and (45). The same comments which were made for the comparison of the experimental and calculated values of ϵ_N in the last section apply here; i.e., the agreement between curve *B* and Eq. (2) is fortuitous.

The Drude model has been shown[13] to describe the spectral absorptivity of Al quite accurately. We compare the experimental and calculated ϵ_H for Al in Fig. 12. The experimental data (the solid dots) fall below ϵ_H calculated with Eq. (2) (Curve *B*) over the entire temperature range. The apparent agreement at low temperatures is again an accident. At low temperatures the relaxation time of the metal is dominated by the Holstein phonon emission process and also by surface scattering. These contributions make the effective relaxation-time temperature independent and much smaller than would be calculated from the dc resistivity alone. Since the black-body spectrum is temperature dependent then at low temperatures the infrared properties of the metal correspond to the region where $\langle\omega\rangle\tau < 1$ in Fig. 3. This is just the regime for which Eq. (2) was derived. Of course the τ in Eq. (2) is incorrect because surface scattering and the Holstein effect are not included. The exact calculation, curve *C*, given by Eq. (45) is also shown for comparison. Only the dc resistivity ρ_μ the Debye temperature, Θ, and r_s are needed for this calculation. Curve *A* gives the low-temperature emissivity calculated with Eq. (58). We would expect that a proper treatment of the low-temperature far-infrared properties of aluminum would produce a curve which would make a smooth transition from curve *A* to curve *C*. The Parker and Abbott

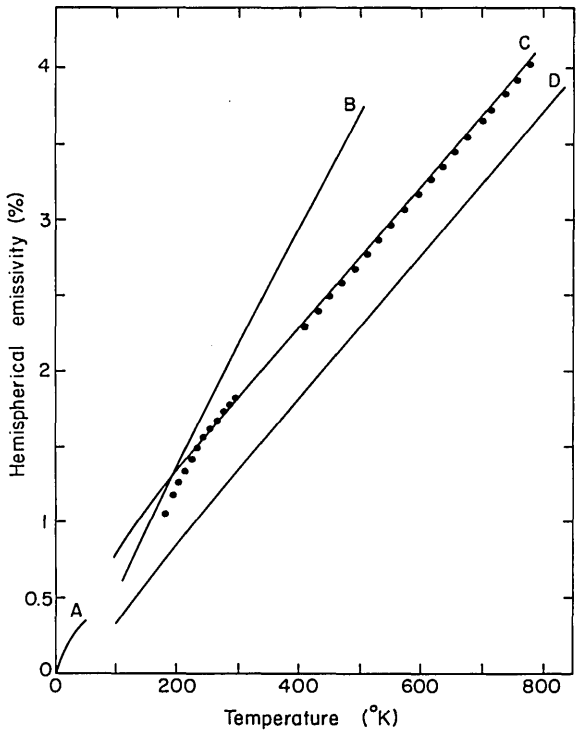

FIG. 12. Experimental and calculated total hemispherical emissivity of aluminum vs temperature. The dots represent the data of Ramanathan *et al.* Ref. 12. Curve (*A*), the extreme anomalous skin effect; curve (*B*) the Davisson-Weeks result [Eq. (2)]; curve (*C*) calculated with Eq. (45) and curve *D*, the Parker-Abbott result (Ref. 6). For curve *C* we have used $r_s/a_0 = 2.17$ as given in Ref. 13.

estimate of the hemispherical emissivity of aluminum, curve *D*, is what Ramanathan *et al.*[12] used to find their anomalous "emissive relaxation times".

IV. Discussion and Conclusions

So far we have developed expressions for the total normal and hemispherical emissivity which have no adjustable parameters and which do not require additional information about the optical properties of metals. We obtained these results by treating only the free carrier or intraband absorption. We now turn to consider model corrections and other absorption processes which are usually identified by spectroscopic measurements. Any frequency dependences associated with such terms would be expected to produce characteristic temperature dependences in the total emissivities beyond those of the free-electron model treated so far.

Band structure is expected to change the calculated emissivities in three important ways:

Firstly, the effective mass, m_{op}, of the free carriers in the Drude model is different from the bare electron mass m. For aluminum [15] $m_{op} = 1.55$ m. This different mass can be inserted into our expressions for ϵ_N and ϵ_H if we replace

$$\rho_\mu(T) \rightarrow \rho_\mu(T)(m/m_{op})^{1/2}.$$

Secondly, the electron-phonon relaxation time in the infrared τ_r is smaller than the time calculated from the dc resistivity τ_{dc} if anisotropic scattering occurs on the Fermi surface.[14] This anisotropy can be inserted into our expressions for ϵ_N and ϵ_H by replacing the correction term above with

$$\rho_\mu(T) \rightarrow \rho_\mu(T)(m/m_{op})^{1/2}\frac{\tau_{dc}}{\tau_{ir}}. \tag{59}$$

This correction applied to Eq. (39) gives the new relaxation frequency. Typically $(m/m_{op})^{1/2} < 1$ while $\tau_{dc}/\tau_{ir} > 1$ so these two correction terms tend to cancel to some extent. τ_{dc}/τ_{ir} is not known for Al but we show in the adjoining paper[38] that for copper the cancellation is almost complete. Also, we expect this correction term to be less important at high temperatures where the periodicity of the lattice is strongly perturbed by temperature and band structure effects tend to wash out.[39]

Thirdly, the onset of interband absorption sets a natural upper limit to the maximum thermal frequency and hence the maximum temperature at which the free-electron model will apply. For many conductors the interband absorption is at frequencies large compared to the thermal radiation frequencies even at the melting point. These interband transitions will still change the infrared emissivity through their effect on the real part of the dielectric constant. Hence the displacement current can no longer be ignored as we did in setting up Eq. (8). If we call the interband contribution to the dielectric constant $\delta\epsilon$, then the real dielectric constant in the displacement current term of Maxwell's equations is $\epsilon = 1 + \delta\epsilon$. In the limit that the conduction current still dominates the displacement current and $\omega\tau > 1$ the surface resistance R_D and reactance, X_D, can be approximated by

$$R_D/Z_0 = (R/Z_0)[1 + (3/2)\epsilon(\omega/\omega_p)^2] \tag{60}$$

and

$$X_D/Z_0 = (X/Z_0)[1 + (\epsilon/2)(\omega/\omega_p)^2], \tag{61}$$

where R and X are given by Eqs. (15) and (16), respectively. The corresponding total normal emissivity is

$$\epsilon_N \approx (2/\omega_p\tau)[g_1(r) + 358\epsilon(m_{op}/m)(c/\omega_p)^2T^2h(r)], \tag{62}$$

where $2/\omega_p\tau$ is given by combining Eqs. (28), (39), and (59), and

$$h(r) = \int_0^\infty x^2 g(x,r)L_x\,dx \Big/ \int_0^\infty x^2 L_x\,dx. \tag{63}$$

The functional dependence of $h(r)$ is shown in Fig. 5 and tabulated in Appendix I.

Within the same limits that we used to derive Eq. (44) (namely, a good conductor) Eq. (62) indicates that the interband contribution to the total emissivity varies with temperature as

$$\Delta\epsilon_N(\text{interband}) \sim T^2\rho_\mu(T). \tag{64}$$

For the noble metals in the near infrared the relaxation time becomes strongly frequency dependent.[40] Only part of this contribution is due to the interband effect described above. The remainder is assigned to electron-electron scattering. An order of magnitude estimate has been made for the electron-electron relaxation time by Gurzhi,[41] who finds that

$$\frac{1}{\tau_{e\text{-}e}} = \omega_p\left[\left(\frac{kT}{\hbar\omega_p}\right)^2 + \frac{1}{4\pi}\left(\frac{\omega}{\omega_p}\right)^2\right]. \tag{65}$$

For good conductors the electron-electron scattering contribution to ϵ_N is

$$\Delta\epsilon_N(e\text{-}e) = 2(c/\omega_p)^2(m_{op}/m)T^2[19.1g_1(r) + 28.6h(r)]. \quad (66)$$

This temperature dependence is quadratic when $r < 2$. Both the interband and the electron-electron contributions are small (less than 2% of the electron-phonon contribution) for good conductors.

Another contribution to the total emissivity of metal surfaces should come from electron scattering due to adsorbed gases. Electrical resistivity measurements of pure and gas covered metallic films[42] with thickness ~100 Å always produce a resistivity increase with increasing coverage of molecules. For example, a 30% increase in the dc resistivity is observed for CO adsorption on 100 Å-thick copper films. Wissman[43] has attempted to explain these results by assuming largely specular scattering of conduction electrons at the clean metal surface and assuming that gas adsorption creates new scattering centers at the film surfaces, similar to the scattering centers produced by alloying foreign atoms in the bulk. A consistant theoretical explanation of the surface resistance changes due to gas adsorption on metal surfaces has not yet appeared. Since the infrared penetration depth is only 100 Å, these dc effects no doubt occur in the infrared as well. No emissivity measurements to date have been made under UHV (ultra high vacuum) conditions so surface layers were present on even the smoothest samples.

In this paper, we have made an exact calculation of the total normal and hemispherical emissivities for free-electron-like metals within the framework of the Drude model. We have found that the Foote expression for ϵ_N and the Davisson and Weeks expression for ϵ_H, which have been widely used in the literature, are unsound. These equations were derived from a limit of the Drude model ($\omega\tau < 1$) which is not appropriate for describing the thermal radiation for most metals at high temperatures.

In our derivation both diffuse surface scattering and electron-phonon scattering have been included. With no adjustable parameters we obtain good agreement with the experimental data for good conductors such as Al. For metals such as Pt and Ta our calculations can only be used to obtain the minimum emissivity since interband transitions no doubt play a larger role here. Within this limitation we have shown that for good conductors, the temperature dependence of both ϵ_N and ϵ_H varies as $\rho_\mu(T)$. We have found two useful approximations for the emmissivities, Eq. (43) for ϵ_N and Eq. (57) for ϵ_H. We have also estimated the form of the different physical processes contributing to the emissivities. For good conductors, we find that for (i) surface scattering, $\Delta\epsilon_N \sim$ const.; (ii) electron-phonon scattering $\Delta\epsilon_N \sim \rho_\mu(T)$; (iii) interband transitions $\Delta\epsilon_N \sim T^2\rho_\mu(T)$; and (iv) electron-electron scattering $\Delta\epsilon_N \sim T^2$. With the aid of a computer it may be possible to unfold the different physical processes contributing to the hemispherical emissivity.

ACKNOWLEDGMENTS

Discussions with A. S. Barker Jr. and R. H. Silsbee have been particularly helpful.

This work has been supported by the Department of Energy Under Contract No. EG-77-S-03-1456. Additional support was received from the National Science Foundation under Grant DMR-76-81083 through the Cornell Materials Science Center, Report #3023.

APPENDIX I

Three overlap integrals have been used in the text. They are $g_1(r)$ defined by Eq. (42), $g_2(r)$ defined by Eq. (55) and $h(r)$ defined by Eq. (63). The values of these functions are tabulated below.

r	$g_1(r)$	$g_2(r)$	$h(r)$
0.15	0.999	0.997	0.999
0.20	0.998	0.996	0.999
0.30	0.995	0.991	0.998
0.40	0.992	0.985	0.997
0.60	0.984	0.969	0.995
0.80	0.975	0.952	0.991
1.0	0.964	0.932	0.987
1.5	0.936	0.881	0.974
2.0	0.907	0.829	0.959
3.0	0.851	0.736	0.925
4.0	0.802	0.656	0.890
6.0	0.720	0.535	0.824
8.0	0.658	0.449	0.767
10.0	0.609	0.387	0.719
15.0	0.521	0.285	0.628
20.0	0.462	0.226	0.563
30.0	0.387	0.159	0.477
40.0	0.339	0.122	0.420
60.0	0.280	0.0839	0.350
80.0	0.244	0.0638	0.306
100	0.219	0.0515	0.275

[1]E. Aschkinass, Ann. Phys. **17**, 960 (1905).
[2]P. D. Foote, Bull. Natl. Bur. Stand. **11**, 607 (1914–15).
[3]B. Donovan, *Elementary Theory of Metals*, (Pergamon, Oxford, 1967), p. 220.
[4]*Thermophysical Properties of Matter*, edited by Y. S. Touloukian, Vol. 7 (Plenum, New York, 1970), p. 24a.
[5]C. Davisson and J. R. Weeks, J. Opt. Soc. Am. **8**, 581 (1924).
[6]W. J. Parker and G. C. Abbott, *Symposium on Thermal Radiation of Solids*, edited by S. Katzoff, (NASA SP-55, 1965), p. 11.
[7]M. Jakob, *Heat Transfer*, (Wiley, New York, 1949), p. 51.
[8]G. A. W. Rutgers, *Handbuch der Physik*, edited by S. Flügge (Springer-Verlag, Berlin 1958), Vol. 26, p. 154.
[9]K. Schocken, *Radiative Transfer From Solid Materials*, edited by H. Blau and H. Fischer (Macmillan, New York, 1962), p. 3.
[10]K. G. Ramanathan and S. H. Yen, J. Opt. Soc. Am. **67**, 32 (1977).
[11]E. A. Estalote and K. G. Ramanathan, J. Opt. Soc. Am. **67**, 39 (1977).
[12]K. G. Ramanathan, S. H. Yen, and E. A. Estalote, Appl. Opt. **16**, 2810 (1977).
[13]H. E. Bennett and J. M. Bennett, *Proceedings of the International Colloquium on Optical Properties, Paris, 1965*, edited by F. Abeles, (North Holland, Amsterdam, 1966), p. 175; H. E. Bennett, J. M. Bennett, E. J. Ashley, and R. J. Motyka, Phys. Rev. **165**, 755 (1968).
[14]J. A. McKay and J. A. Rayne, Phys. Rev. B **13**, 673 (1976).
[15]N. W. Ashcroft and K. Sturm, Phys. Rev. B **3**, 1898 (1971).
[16]B. Donovan, *Elementary Theory of Metals*, (Pergamon, Oxford, 1967), p. 215.
[17]L. D. Landau and E. M. Lifshitz, *Electrodynamics of Continuous Media* (Addison-Wesley, Reading, Massachusetts, 1960), p. 280.
[18]A. B. Pippard, *Optical Properties and Electronic Structure of*

Metals and Alloys, edited by F. Abeles (North Holland, Amsterdam, 1966) p. 622.
[19]F. J. Blatt, *Physics of Electronic Conduction in Solids* (McGraw-Hill, New York, 1968), p. 194.
[20]N. F. Mott and H. Jones, *The Theory of the Properties of Metals and Alloys,* (Dover, New York, 1936), p. 268.
[21]N. W. Ashcroft and N. D. Mermin, *Solid State Physics,* (Holt, Rinehart and Winston, New York, 1976), p. 5, (see Appendix A for numerical relations between τ, ρ_μ, r_s/a_0, v_F, *and* ω_p).
[22]Ref. 20, Appendix II, p. 318.
[23]G. E. H. Reuter and E. H. Sondheimer, Proc. Roy. Soc. A **195,** 336 (1948).
[24]T. Holstein, Phys. Rev. **88,** 1427 (1952).
[25]R. B. Dingle, Physica **19,** 311 (1953).
[26]A. B. Pippard, *in Advances in Electronics and Electron Physics,* edited by L. Marton, (Academic, New York, 1954), p. 1.
[27]H. B. G. Casimir and J. Ubbink, Philips Tech. Rev. **28,** 300 (1967).
[28]F. Wooten, *Optical Properties of Solids,* (Academic, New York, 1972), p. 93.
[29]The positions of the boundaries change slightly from metal to metal since they depend on relaxation time and the electron density. See Ref. 28 for a complete description of the boundary parameters.
[30]T. Holstein, Ann. Phys. (N.Y.) **29,** 410 (1964); Phys. Rev. **96,** 535 (1954).
[31]R. N. Gurzhi, Zh. Eksp. Teor. Fiz. **33,** 660 (1957) [Sov. Phys. JETP **6,** 506 (1958)]; **35,** 965 (1958) [Sov. Phys. JETP **8,** 673 (1959)].
[32]For Cu, Pt, and Ag, $\rho_\mu(T)$ was taken from *American Institute of Physics Handbook,* 3rd Edition, McGraw Hill, New York) while for the rest of the elements ρ_μ(T) was taken from *Metals Reference Book* Vol. III, edited by C. J. Smithells, (Butterworths, London, 1967). Values of r_s were taken from Ref. (20) or (21).
[33]G. L. Abbott, in *Measurement of Thermal Radiation Properties of Solids,* edited by J. C. Richmond, (NASA SP-31, 1963), p. 293.
[34]R. Blickensderfer, D. K. Deardorff, and R. L. Lincoln, J. Less-Common Metals **51,** 13 (1977).
[35]G. A. Zhorov, High Temp. **5** 881 (1967) [English translation of Teplofiz, Uys. Temp., **5,** 987 (1967)].
[36]H. T. Betz, O. H. Olson, B. O. Schurin, and J. C. Morris, *Determination of Emissivity and Reflectivity Data on Aircraft Structural Materials,* Pt. 2, AD 202493, 1958.
[37]D. S. Jones, *The Theory of Electromagnetism* (Pergamon, Oxford, 1964), p. 322.
[38]R. Smalley and A. J. Sievers, J. Opt. Soc. Am. **68,** 1516–1518 (1978).
[39]A. G. Mathewson and H. P. Myers, J. Phys. F. Metal Phys. **3,** 623 (1973).
[40]R. T. Beach and R. W. Christy, Phys. Rev. B **16,** 5277 (1977).
[41]R. N. Gurzhi, M. Y. Azbel, and H. P. Lin, Fiz. Tverd. Tela. **5,** 759 (1963) [Sov. Phys. - Solid State **5,** 554 (1963)].
[42]R. Suhrmann, H. Ober, and G. Wedler, Z. Phys. Chem. (Frankfurt) **29,** 305 (1961).
[43]P. Wissmann, in *Springer Tracts in Modern Physics 77,* edited by G. Höhler (Springer-Verlag, New York, 1975), p. 1.

The total hemispherical emissivity of copper

R. Smalley and A. J. Sievers
Laboratory of Atomic and Solid State Physics and Materials Science Center, Cornell University, Ithaca, New York 14853
(Received 17 May 1978)

The transient calorimetric technique is used to measure the temperature dependence of the total hemispherical emissivity of polished copper. Our experimental results do not agree with the emissivity predicted by Parker and Abbott. With no adjustable parameters good agreement is obtained between experimental results and a model in which electron-phonon and electron-surface scattering are included in the Drude approximation.

I. INTRODUCTION

For metals which are good electrical and thermal conductors, the Drude free-electron model combined with Maxwell's equations can be used to calculate the absorptivity and emissivity of metal surfaces. Davisson and Weeks[1] first applied this approach but used the Hagen-Rubens relation (the Drude model in the limit $\omega\tau \ll 1$) to describe the infrared properties of metals. In this way, they were able to relate the total thermal radiation from a metal to the bulk resistivity and the temperature. More recently Parker and Abbott[2] included finite relaxation-time effects and constructed five different equations for the hemispherical emissivity for five different relaxation parameters. One of these equations which was appropriate for copper was

$$\epsilon_H = 0.281\,(\rho T)^{1/2} - (0.153 - 0.0109\ln\rho T)\rho T + 0.0461\,(\rho T)^{3/2}, \quad (1)$$

where ρ is the electrical resistivity in Ω cm and T is the temperature in (°K). This equation has the same form as the original Davisson-Weeks equation but the numerical coefficients depend on the relaxation parameter of the metal.

Over the years a number of experiments have been compared with the Davisson-Weeks expression.[3] Early experiments appeared to confirm this relation while more recent measurements by Ramanathan and coworkers[4,5] strongly disagree not only with the Davisson-Weeks equation but also in the case of copper, with Eq. (1) above.[6]

In this paper, we report on our measurement of the temperature dependence of total hemispherical emissivity of copper. Good agreement is found between our measurements and those of Ramanathan and Yen.[4] We then compare our measured results with an exact calculation of the hemispherical emissivity using a model in which electron-phonon and electron-surface scattering are included in the Drude approximation. This model is described in the adjoining paper[7] which we shall refer to as I. Good agreement between experiment and this model is found with no adjustable parameters.

II. EXPERIMENTAL TECHNIQUE

The transient calorimetric technique offers a relatively simple way to measure a specimen's total hemispherical emittance. In this technique a thermally isolated sample, not in thermal equilibrium with its surroundings, is brought to

 0030-3941/78/6811-1516$00.50